Journal of Energy Chemistry 27 (2018) 1198–1207

Contents lists available at ScienceDirect

Journal of Energy Chemistry

journal homepage: www.elsevier.com/locate/jechem

http://www.journals.elsevier.com/journal-of-energy-chemistry/

Rheological properties and viscosity reduction of South China Sea crude oil

Hui Sun[a,*], Xingxing Lei[a], Benxian Shen[a], Huiran Zhang[a], Jichang Liu[a], Gengnan Li[b], Di Wu[b,c,d,**]

[a] Petroleum Processing Research Center, East China University of Science and Technology, Shanghai 200237, China
[b] The Gene and Linda Voiland School of Chemical Engineering and Bioengineering, Washington State University, Pullman, WA 99163, United States
[c] Department of Chemistry, Washington State University, Pullman, WA 99163, United States
[d] Materials Science and Engineering, Washington State University, Pullman, WA 99163, United States

ARTICLE INFO

Article history:
Received 8 June 2017
Revised 25 July 2017
Accepted 28 July 2017
Available online 8 August 2017

Keywords:
South China Sea crude oil
Characterization
Rheological properties
Viscosity reduction

ABSTRACT

The rheological properties of South China Sea (SCS) crude oil were studied. A group of synthetic long-chain polymers, including octadecyl acrylate-maleic anhydride bidodecyl amide copolymer (VR-D), octadecyl acrylate-maleic anhydride bioctadecyl amide copolymer (VR-O) and octadecyl acrylate-maleic anhydride phenly amide copolymer (VR-A), were employed to serve as viscosity reducers (VRs). Their performance was evaluated by both experimental and computational methodologies. The results suggest that the SCS crude oil has low wax content yet high resin and asphaltene contents, which lead to high viscosity through formation of association structures. Additionally, the SCS crude oil appears to be a pseudoplastic fluid showing linear shear stress-shear rate dependence at low temperature. Interestingly, it gradually evolves into a Newtonian fluid with exponential relationship between shear stress and shear rate at higher temperature. Synthetic VRs demonstrate desirable and effective performance on improvement of the rheological properties of SCS crude oil. Upon the introduction of 1000 ppm VR-O, which is synthesized by using octadecylamine in the aminolysis reaction, the viscosity of SCS crude oil is decreased by 44.2% at 15 °C and 40.2% at 40 °C. The computational study suggests significant energy level increase and shear stress decrease for VR-containing crude oil systems.

© 2017 Science Press and Dalian Institute of Chemical Physics, Chinese Academy of Sciences. Published by Elsevier B.V. and Science Press. All rights reserved.

1. Introduction

The increasing demand of petroleum results in an increasing exploitation and production of crude oil resources, among which the heavy oil resources in the world are at least twice as many as those of conventional light crude oil. Heavy and extra-heavy crude oil refining poses enormous challenges in the pipeline transportation of petroleum liquids. One critical issue is their high viscosity and low fluidity, which are governed by their fundamental physical and chemical properties such as oil compositions (i.e., saturates, aromatics, resins and asphaltenes, traces of sulfur, nitrogen, chlorine and metal compounds), and the complicated interactions among different oil species [1–4]. Generally, waxes, paraffins with high melting points, are mainly responsible for the low-temperature flow issues of waxy crude oils. In addition, high resin and asphaltene contents also lead to undesirable rheological properties and reduced mobility, causing precipitation, emulsification, high viscosity, equipment corrosion and coking deactivation of catalysts in numerous processes of the petroleum industry [5–7]. Therefore, knowing the fundamental properties of resins and asphaltenes is very important for evaluating and predicting their impacts on crude oils refining and process design and optimization.

Resins and asphaltenes can be separated from petroleum sources. Their structures have been studied by both experimental characterization techniques [8–11] and theoretical calculations [12,13]. Typically, resin and asphaltene molecules tend to form association structures, which lead to crude oils with very high viscosity [14–16]. The major forces governing the resin and asphaltene aggregates formation are very complicated, including charge transfer, electrostatic interaction, van der Waals force, the acid-base interaction, hydrogen bonding, $\pi-\pi$ interaction and coordination interaction [17–20].

* Corresponding author.
** Corresponding author at: The Gene and Linda Voiland School of Chemical Engineering and Bioengineering, Washington State University, Pullman, WA 99163, United States.
E-mail addresses: sunhui@ecust.edu.cn (H. Sun), d.wu@wsu.edu (D. Wu).

http://dx.doi.org/10.1016/j.jechem.2017.07.023
2095-4956/© 2017 Science Press and Dalian Institute of Chemical Physics, Chinese Academy of Sciences. Published by Elsevier B.V. and Science Press. All rights reserved.

It has been reported that polymers, graphene, graphene oxide (GO) and reduced GO could reduce the viscosity of fluids [21–25]. To reduce the viscosity and to improve the fluidity of crude oils and heavy petroleum fractions, one approach is to break or disperse the asphaltene-resin-involved association aggregates using various additives, such as synthetic viscosity reducers (VRs) [26,27], lighter blending components [28], electric or magnetic fields [29,30], heterogeneous catalysts [31,32], and nanoparticles [33]. A spectrum of polymers has also been synthesized to improve the fluidity [34–37]. These methods exert significant impact on the complex aggregates, lowering the viscosity and yield stress of crude oil and enabling much easier flow and transportation.

It is fundamentally crucial and practically necessary to investigate the physical and chemical properties of crude oil, which govern its application in the petroleum industry. Huge oil reserves were found in the South China Sea (SCS), which greatly boosts the research on this unique oil source. In this work, we focused on the rheological behaviors and viscosity reduction of SCS crude oil. The properties of SCS crude oil sample, especially its rheological properties, were thoroughly characterized. Moreover, a series of nitrogen-containing long-chain polymers were synthesized and employed to serve as the VRs. Furthermore, the rheological property evolution of SCS crude oil upon VR introduction was evaluated via both experimental and computational methodologies.

2. Experimental

2.1. Materials

Crude oil obtained from the South China Sea oil field was used in this work. Other chemicals used were of analytical grade and were used as received without any further treatment. The chemicals and corresponding suppliers are listed below. Methanol and acrylic acid were obtained from Shanghai Titan Scientific Co., Ltd. (Shanghai, China). Toluene, sodium hydroxide, *p*-toluene sulfonic acid, *cis*-butenedioic anhydride and hydroquinone were provided by Shanghai Lingfeng Chemical Reagent Co., Ltd. (Shanghai, China). Benzoyl peroxide, vinyl acetate, dodecylamine, octadecylamine, aniline and dodecyl mercaptan were purchased from Sinopharm Chemical Reagent Co., Ltd. (Shanghai, China). 1-Octadecanol was obtained from Yonghua Special Chemical Reagent Company (Taicang, Jiangsu).

2.2. Synthesis of viscosity reducers (VRs)

2.2.1. Esterification reaction

Esterification reaction of 1-octadecanol (OD) and acrylic acid (AA) was carried out in a three-necked flask reactor under constant magnetic stirring at 125 °C for 8 h (Scheme 1). The reaction temperature was accurately controlled by using an oil-bath heater, in which toluene (T), *p*-toluene sulfonic acid (SA) and hydroquinone (HQ) were used as solvent, catalyst and polymerization inhibitor, respectively. Specifically, the starting mixture had a molar composition of n(OD):n(AA):n(T) = 1:1.3:2.3. The corresponding mass ratios, m(SA)/m(OD+AA) and m(HQ)/m(OD+AA), were 0.007 and 0.01, respectively. Subsequently, the resulting product, octadecyl acrylate, was washed with sodium hydroxide aqueous solution (5 wt%) and thereafter deionized water followed by vacuum drying at 50 °C for 4 h.

2.2.2. Polymerization reaction

Vinyl acetate (VA), *cis*-butenedioic anhydride (BDA) and synthesized octadecyl acrylate (ODA) in the esterification reaction were used as monomers for copolymerization, which was performed in a three-necked flask heated in an oil-bath under N_2 environment (80 mL min^{-1}). The reaction is detailed in Scheme 2. Toluene (T), benzoyl peroxide (BPO) and dodecyl mercaptan (DM) were used as solvent, polymerization initiator and chain-transfer agent, respectively. The starting mixture had a molar composition of n(VA):n(BDA):n(ODA):n(T) = 1:1:4:12. Both benzoyl peroxide and dodecyl mercaptan account for 3% of the total mass of reactants (VA, BDA and ODA). The polymerization reaction was maintained to be under 100 °C under constant mechanical stirring for 6 h. Subsequently, the polymerization product mixture was transferred into a beaker containing methanol to stop the reaction and to enable precipitation of the copolymer. Finally, the solid product was separated through filtration and dried under vacuum at 50 °C for 4 h.

2.2.3. Aminolysis reaction

Three VRs were synthesized through aminolysis reaction. The synthesized polymer reacted with dodecylamine (D), octadecylamine (O) and aniline (A), forming three groups of VRs labeled as VR-D, VR-O and VR-A, respectively (see Scheme 3). The aminolysis reactions was conducted in a three-necked flask containing toluene solvent, which was kept at 90 °C for 6 h under N_2 flow (80 mL min^{-1}). Upon aminolysis, the synthesized products were separated through filtration and dried under vacuum for 4 h.

2.3. Analyses and measurements

2.3.1. Characterizations

A series of crude oil characteristics, including water content, wax content, SARA (referring to Saturates, Aromatics, Resins and Asphaltenes, respectively) distribution, API gravity and freezing point, were determined using Chinese National Standard Test Method (CNSTM), Chinese Petroleum Standard Test Method (CPSTM) and ASTM standard test method.

The wax content of crude oil was determined according to the method recommended by Baudilio et al. [38]. Approximately 2 g of SCS crude oil was dissolved in 40 mL of *n*-pentane followed by addition of 120 mL acetone. Subsequently, this mixture was cooled to −20 °C and kept for 24 h. Further, the solid phase was separated through filtration. The wax product was obtained by redissolvation of the solid phase in *n*-hexane followed by solvent removal.

The SARA distribution was determined by using ASTM D2007-93 standard test method. Firstly, asphaltenes and resins were isolated through precipitation in *n*-hexane solvent with a solvent to crude oil ratio of 30 by volume. Upon cooling to −30°C, asphaltenes were separated via filtration. The obtained solid asphaltenes were further washed with *n*-heptane and dried under vacuum. Subsequently, the liquid phase (maltene fraction) was separated into saturated hydrocarbons, aromatics, and resins by applying a standard chromatographic process. Specifically, the chromatographic separation was carried out using a glass column packed with alumina (100–200 mesh, Sinopharm, China). Trichloromethane, *n*-hexane and toluene were employed to recover resins, saturates, and aromatics at a Soxhlet apparatus, respectively. The contents of SARA can be calculated according to the amount recovered [39].

The water content of all samples was analyzed according to the CNSTM GB/T 8929-2006. The API gravity of each sample was estimated from its specific gravity value measured at 40 °C using a pycnometer based on CNSTM GB/T 1884-2000. The freezing point was determined by using a SYP1008-III freezing point analyzer (Shanghai Petroleum Instruments Company, Shanghai, China) according to CPSTM SY/T 0541-2009. The test tube containing sample was cooled at 0.5–1.0 K min^{-1}. Each measurement was repeated for 2–3 times to ensure reproducibility.

2.3.2. Rheology tests

All rheology tests were performed using a MCR-52 rotary rheometer (Anton Paar, Physica, Austria) equipped with a stainless

steel cup geometry CC27. RHEOPLUS/32 O+R (Version 3.62) (Anton Paar, Physica, Austria) workstation was used for data processing. For flow pattern determination, the sample was cooled below 10 °C and then heated from 10 to 80 °C stepwisely with an interval of 5 °C. At each temperature, the shear rate (γ, s^{-1}) was increased from 1 to 100 s^{-1} within 1400 s. The rheological curves data of crude oil were collected at different temperature. On the other hand, to measure the critical stress and thixotropy, the crude oil sample was heated to 60 °C, kept for 10 min and then cooled to 15 °C at 1 °C min^{-1}. In the critical stress measurement, the viscosity value (μ, Pa s) was recorded as shear stress (τ, Pa) evolved from 0 to 1200 Pa. For thixotropy measurement, the sample was sheared from 0 to 20 s^{-1} within 20 min with shear rate increasing linearly. This was followed by shear rate reducing from 20 to 0 s^{-1} linearly within 20 min.

To evaluate the viscosity reduction performance, a fixed amount of VR was added into the crude oil sample. This mixture was maintained at 60 °C for 30 min under moderate stirring. Based on our optimized results, the VR mass concentration in crude oil was set to be 1000 ppm. The VR-containing crude oil sample was cooled to room temperature before the rheological property tests using the same rheometer.

2.3.3. FTIR analyses

FTIR spectra were collected on a Spectrum 100 FTIR Spectrometer (PerkinElmer, Branford, CT, USA). Samples were scanned in the range of 4000–400 cm^{-1} at 4 cm^{-1} interval.

2.3.4. Gel permeation chromatography (GPC) analyses

The molecular weight of synthetic VR was measured using a PL-GPC 50 instrument (Agilent Technologies, Edinburgh, UK). Analyses were carried out at 35 °C, in which each sample was diluted to 5000 ppm using tetrahydrofuran as solvent.

2.3.5. Differential scanning calorimetric (DSC) analyses

Low temperature DSC experiments were performed to investigate the VR-crude oil interactions, motion and potential phase transition-like behaviors for the crude oil. Similar experimental approach was used in an earlier study on vinyl ester resin curing process for polymer nanocomposite fabrication by Guo et al. [40]. Specifically, a Netzsch DSC 200F3 (Netzsch, Selb, Germany) system was employed to carry out the DSC analyses. Prior to each experiment, about 20 mg sample was placed in a Pt crucible and cooled below 10 °C. In each measurement, the sample was heated from 10 to 80 °C at 2 °C min^{-1} under argon flow (40 mL min^{-1}).

3. Density functional theory (DFT) calculation

Density functional theory calculation has been applied extensively to study polymer-based composite materials [41–45]. Here, we employed DFT to investigate the VR-resin and VR-asphaltene interactions. All simulation calculations were performed by using Materials Studio DMol^3 program (Accelrys Software Inc.). The detailed simulation process is described in Fig. 1.

4. Results and discussion

4.1. Characterization of crude oil

The properties of SCS crude oil are summarized in Table 1, which strongly suggests that SCS crude oil is classified as heavy crude oil (API gravity of 11.4). Compared with several other types of crude oil including Maya crude oil [46], Indian (Bombay High, Moran, and Geleki) crude oil [26,27] and Brazilian waxy crude oil [47], SCS crude oil has lower wax content (1.6%) and higher resin content (39.3%), which leads to its low freezing point and high viscosity, respectively. In our previous study, the structures of both resin and asphaltene in SCS crude oil were determined through integration of multiple analytical techniques [48]. Table 2 summarizes the average structural parameters of resin and asphaltene molecules in SCS crude oil we obtained. Based on these structural parameters, we were able to generate the model molecules of resin and asphaltene (see Fig. 2).

Table 1. Properties of SCS crude oil.

Properties	Observed values
API	11.4
Freezing point (°C)	23
SARA distribution (wt%)	
Saturates	20.7
Aromatics	33.1
Resins	39.3
Asphaltenes	3.9
Recovery rate	97
Wax content (wt%)	1.6
Water content (wt%)	4.2

4.2. Synthesis of VRs

Under the reaction conditions described (see Section 2.2), the conversions are 90.84% and 78.45% for esterification and polymerization reactions, respectively. GPC analysis suggests that the polymerized product has an average molecular weight of 5318 g mol^{-1}, which is in the typical range of VRs [26].

FTIR spectra of synthesized VRs (VR-D, VR-O and VR-A) are presented in Fig. 3. The peak at 1680 cm^{-1} is assigned to the N–H in-plane bending vibration of primary amide group, while the signal at 1200 cm^{-1} is attributed to C–O–C asymmetrical stretching vibration of ester group. The peaks at 2851.97 and 2922.19 cm^{-1} correspond to the symmetrical and asymmetrical stretching vibration of methylene group. For VR-A, the signals for C=C stretching vibration at 1601–1496 cm^{-1} and =C–H out-of-plane bending vibration at 2042–1857 cm^{-1} are due to phenyl group insertion.

4.3. Rheological properties of SCS crude oil and viscosity reduction

4.3.1. Viscosity-temperature dependence

The relationship among temperature, shear rate γ and dynamic viscosity μ is illustrated as a 3D graph in Fig. 4(a). There appears to be a damping descending rate of μ as either temperature or γ increases. As temperature reaches 30 °C, μ stays within the same plane (surface) upon γ increasing. The viscosity–temperature relationship for crude oil samples with and without VRs was studied under a constant shear rate γ of 10 s^{-1} (see Fig. 4b). For the parent crude oil sample, below 25 °C, strong temperature dependence of dynamic viscosity was observed due to the formation of stable association structures originated from intermolecular interactions of resin and asphaltene [16,19,49,50]. As temperature increases, the association interactions become weaker, resulting in abrupt decrease in viscosity and less significant temperature dependence. Compared with the parent crude oil, all three VR-containing samples show remarkably reduced viscosity at below 40 °C. This is clearly observed on the viscosity–temperature curves. Owing to their long side chains and polar functional groups, VRs can reduce the association interactions among molecules in crude oil system through inserting into, breaking and then dispersing the association structures. VR-O has the longest side chains, and hence, exhibits slightly better viscosity reduction performance compared with VR-A and VR-D. At 15 and 40 °C, the viscosity reduction rates of VR-O are found to be 44.2% with viscosity decreasing from 375.0 to 209.1 Pa s, and 40.2% with viscosity decreasing from 13.2 to

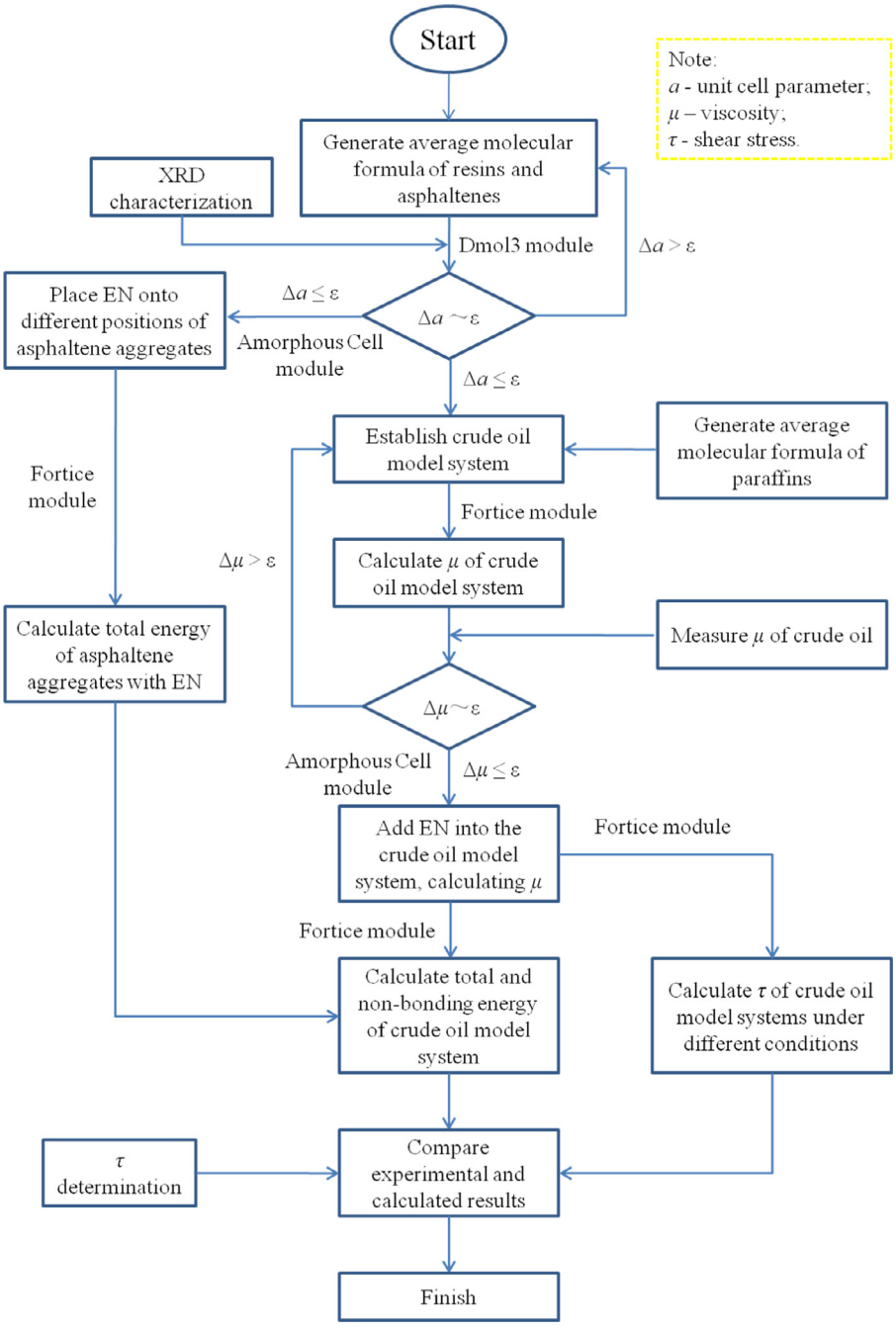

Fig. 1. The simulation flowsheet.

7.9 Pa s (see Fig. 4c). Generally, as temperature increases from 15 to 40 °C, the viscosity reduction rate decreases first followed by sharp slope switch to be positive. Indeed, the initial viscosity reduction rate decrease is largely due to disaggregation effect on the association structures upon temperature increase. On the other hand, the subsequent increase in viscosity reduction rate at above 22 °C is mainly because higher temperature can trigger stretching of the long side chains of VRs, which further insert into the association structures.

Typically, crude oil exhibits three forms of flow as temperature evolves: Newtonian, pseudoplastic and plastic fluids (Fig. 4d). High temperature leads to a Newtonian fluid, which features a linear relationship between shear stress τ and shear rate γ. Temperature decrease leads to association of resin and asphaltene, which results in pseudoplastic flow showing exponential τ vs. γ correlation. Upon further temperature depression, crude oil finally becomes plastic fluid, which only starts moving when reaching a constant shear stress τ_0. According to the non-linear least squares analysis on the τ–γ relationship, the SCS crude oil can be classified as Newtonian fluid from 30 to 85 °C, while it is pseudoplastic fluid for VR-free crude oil, and Bingham fluid for crude oil containing VR-O at temperature between 15 and 25 °C (see Fig. 4d). For VR-free crude oil, the τ–γ relations are found to be $\tau = 11.15\gamma$ at 30 °C and $\tau = 49.10\gamma^{0.87}$ at 25 °C. For crude oil containing VR-O, the τ–γ relationships are $\tau = 71.69 + 9.94\gamma$ at 30 °C and $\tau = 55.91\gamma^{0.77}$ at 25 °C.

Additionally, the DSC curves of crude oil samples with and without VR-O are presented in Fig. 5. As temperature decreases from 35 to 15 °C, the VR-free crude oil shows one wide endothermic peak at 29 °C, whereas the sample containing VR-O presents

Table 2. Observed average structural parameters for resin and asphaltene molecules in SCS crude oil [48].

Parameters	Determination method	Observed values	
		Resins	Asphaltenes
MW ($g\,mol^{-1}$)	Ail[a]	760	1129
Element composition (%)			
C		86.43	88.27
H	Elemental analysis	10.40	9.21
N		0.90	0.42
S		0.86	0.97
O		1.51	1.13
Functional group	IR	Methyl, methylene, acromatic, carboxyl	Methyl, methylene, acromatic, carboxyl
Elemental type			
C		C–C	C–C
N	XPS	Pyrrole	Pyrrole
S		Thioether	Thiophene
O		Carbonyl, carboxyl	Carbonyl, carboxyl
Structural parameters			
Number of AR	UV	3	3, 4, and 5
Aromatic skeleton		Biphenyl, cata-condensed	Cata-condensed, peri-condensed
H_A[b]		10	21
H_α	^{1}H NMR	8	9
H_β		44	46
H_γ		14	24
C_A[c]	^{13}C NMR	22	45
C_S[d]		33	40
C_p/C_n[e]	DEPT 135°	85/15	90/10
d_m[f]		4.13	4.12
d_γ[g]	XRD	5.16	5.15
L_c[h]		21.56	23.56
L_a[i]		43.60	48.17

[a] Referring to reference [55].
[b] Aromatic H.
[c] Aromatic C.
[d] Saturated C.
[e] Ratio of paraffin C (C_p) to naphthenic C (C_n).
[f] Interlamellar spacing.
[g] Chain space.
[h] Height of unit cell.
[i] Interlamellar diameter.

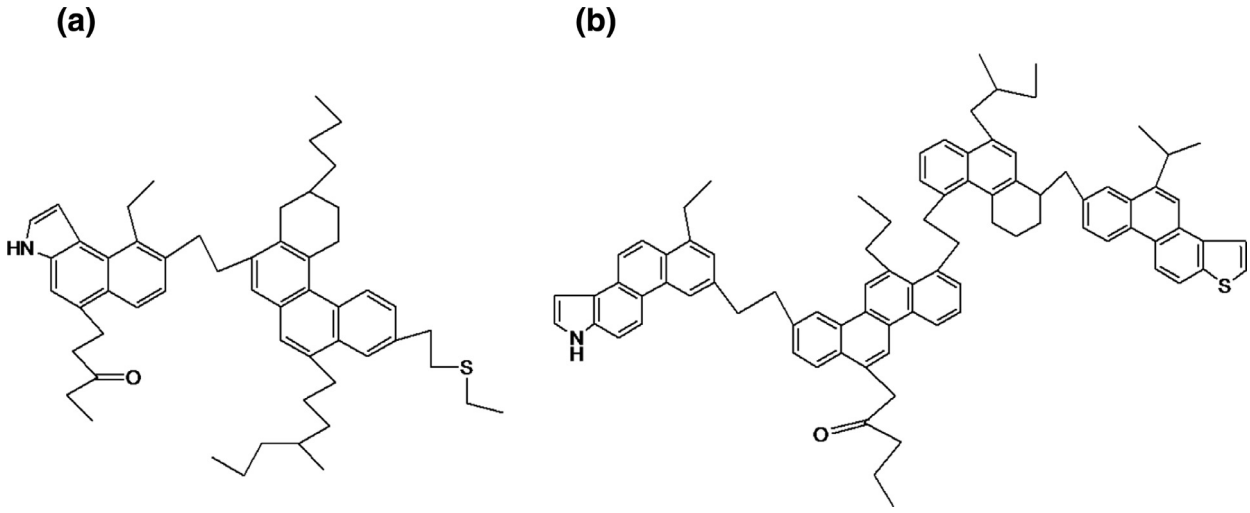

Fig. 2. Average molecules of (a) resin and (b) asphaltene of SCS crude oil.

two endothermic peaks at 22 and 27.5 °C, respectively. The relative high-temperature (27.5 °C) and low-temperature (22 °C) heat events can be attributed to the phase transition and motion increase of micro and the bulk wax crystals in the crude oil, respectively.

At high-temperature, wax crystals precipitate from the liquid. Meanwhile, the crude oil system retains its liquid phase due to inhibition effect of VR-O on both nucleation and growth of wax crystals. Further temperature decreases the bulk crude oil phase transition follows the aggregation of wax crystals. However, we also observed that the VR-O containing crude oil has lower phase transition temperature (freezing point at 20 °C) compared with that of the VR-free crude oil (freezing point at 23 °C), indicating that VR-O may also reduce the pour point of SCS crude oil.

4.3.2. Critical stress measurement

The relationship between μ and τ of SCS crude oil is plotted in Fig. 6(a), suggesting that there is no abrupt change for viscosity at a particular shear stress. At low τ value, μ presents a relative high plateau at about 1070 Pa s. It then becomes less viscous continuously as τ increases from 300 to 1000 Pa. Once τ is over 1000 Pa,

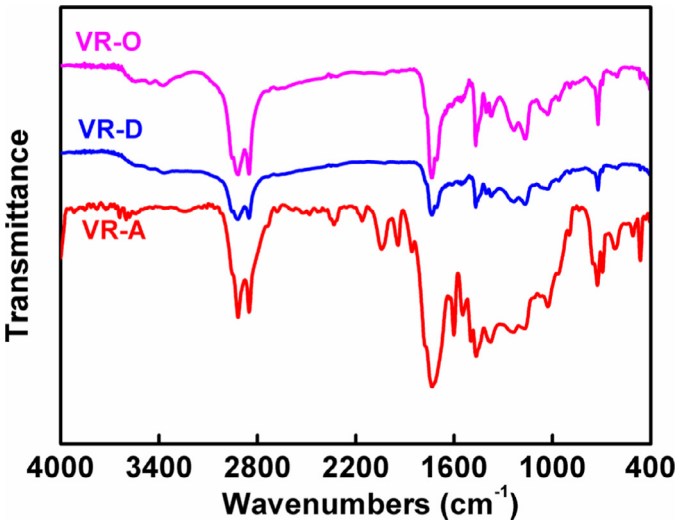

Fig. 3. FT-IR spectra of synthesized VR-D, VR-O and VR-A.

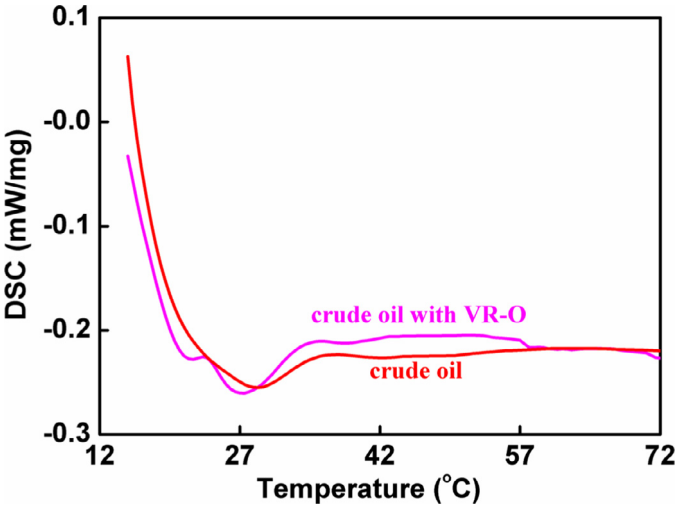

Fig. 5. DSC traces of SCS crude oil samples.

μ reaches the second plateau. According to the $d\mu/d\tau$ curve, the critical stress is found to be 590 Pa. Typically, unlike high-waxy crude oils, SCS crude oil has low wax content. Hence, its low viscosity is mainly determined by the association structures of resin and asphaltene rather than the wax precipitation. These association structures are more difficult to be disassembled and therefore can retain within a wide range of τ. Consequently, SCS crude oil does not present any abrupt decrease of viscosity as shear stress increases. After adding VR-O, the viscosity of crude oil is greatly reduced at low shear stress. By contrast, μ exhibits a low plateau at about 300 Pa s at small τ. Meanwhile, the critical stress decreases from 590 to 370 Pa (see Fig. 6b), suggesting significantly positive effect of VR-O addition to the rheological behavior of SCS crude oil.

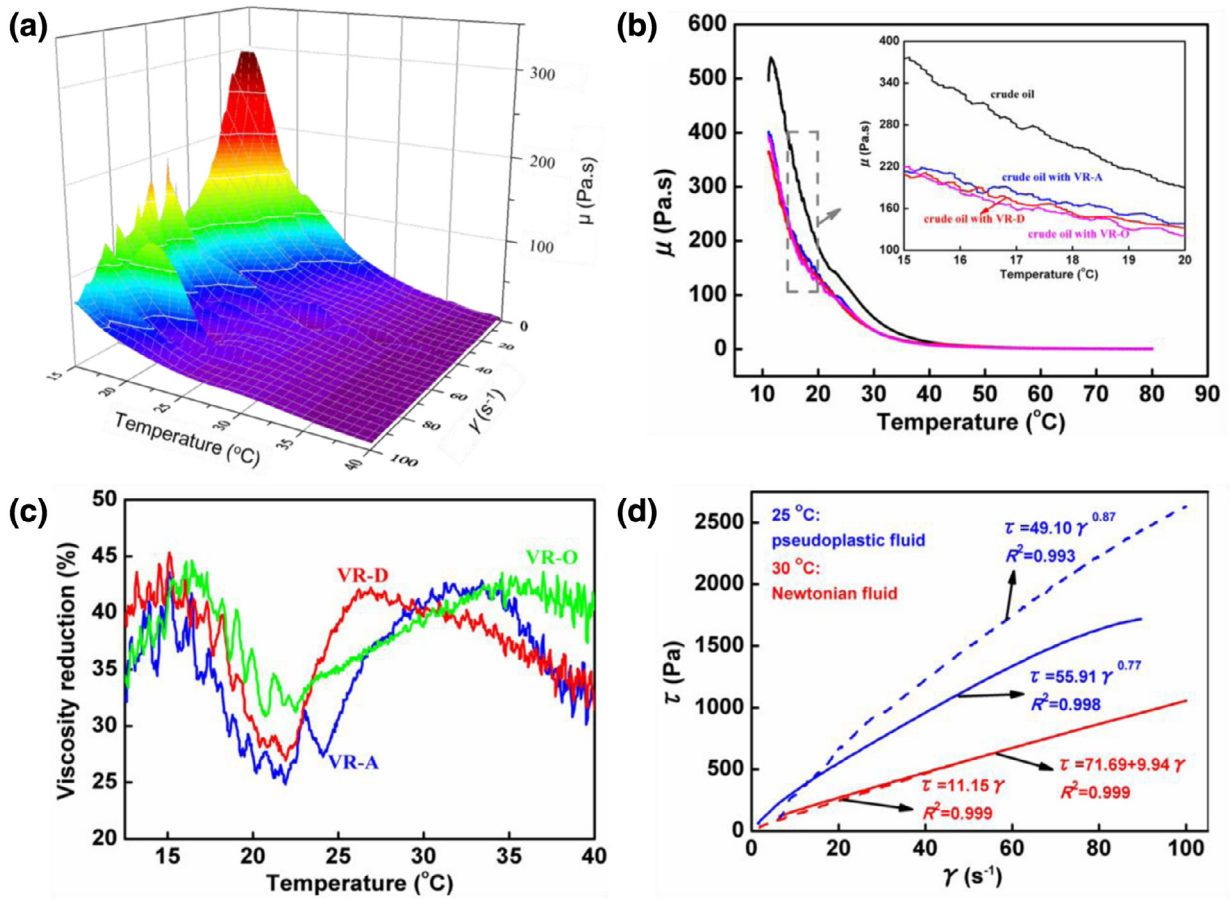

Fig. 4. (a) 3D image of temperature-shear rate-viscosity relationships for SCS crude oil, (b) viscosity of SCS crude oil as a function of temperature (at a constant shear rate γ of 10 s^{-1}), (c) viscosity reduction (%) as temperature varies, (d) rheological properties of SCS crude oil (dashed lines: crude oil without VR-O; solid lines: crude oil with VR-O).

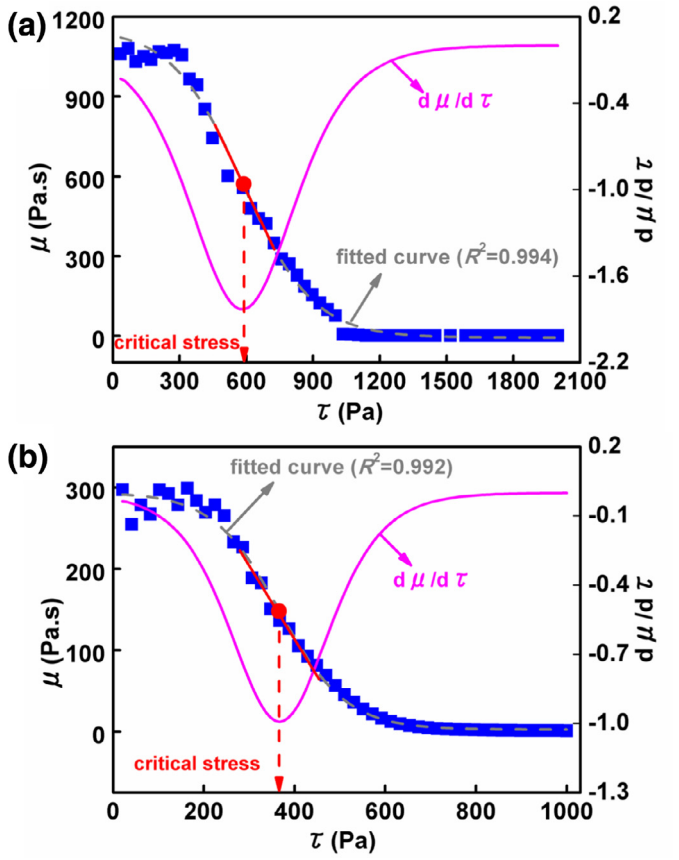

Fig. 6. The viscosity of SCS crude oil as a function of shear stress (a: crude oil without VR-O; b: crude oil with VR-O).

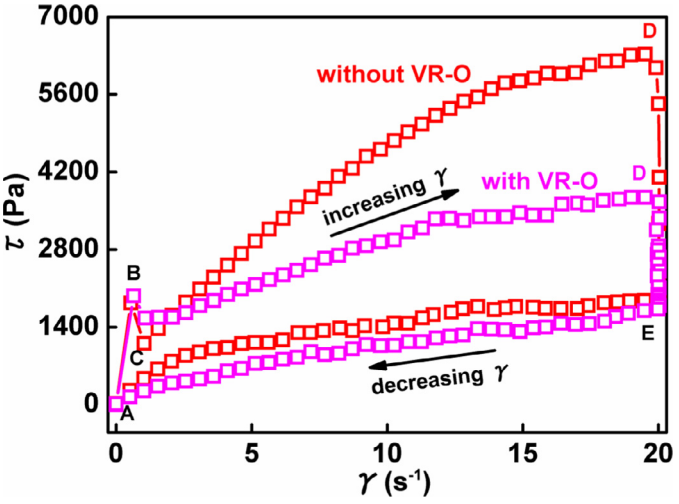

Fig. 7. Hysteritic curves of SCS crude oil.

4.3.3. Thixotropy measurement

The thixotropy of SCS crude oil was investigated by measuring its hysteritic curves at 15 °C (see Fig. 7). It is clearly shown that the crude oil possesses thixotropy. Specifically, the measurement procedure can be described as five distinct steps [51]. Firstly, as the shear rate γ increases from 0 s^{-1} (A), τ increases sharply until reaching a maximum at 1837 Pa (B) indicating formation of stable association structures in crude oil. Subsequently, the crude oil sample begins to flow with increasing γ and descending τ until reaching point (C). Continuing increase of γ leads to τ re-increase until reaching point (D), after which the crude oil sample was sheared for 5 min at the maximum shear rate γ_D of about 20 s^{-1}. Subsequently, τ shows a sharp decrease from 6324 to 1910 Pa, dropping from D to E. Such phenomenon suggests that the association effect is diminished under strong shear condition. Finally, τ gradually decreases to 0 Pa, back to point (A) upon γ decreases. Integration of the closed hysteritic curves is 56,093 Pa s^{-1}. Compared with the parent crude oil, the VR-O containing sample shows much lower τ at γ_D. In other words, point (D) shifts to a lower τ. However, both parent and VR-O containing crude oil samples have nearly the same (E) position. It is very likely that shearing crude oil sample VR-O may weaken the association interactions by disassembling association structures. As a result, the variation magnitude of τ due to increasing γ is narrower. Therefore, a much smaller hysteritic circle area, 35,268 Pa s^{-1}, is observed for the VR-O-containing sample, indicating significant impact of VR-O introduction on the thixotropy of SCS crude oil.

4.4. DFT calculation for crude oil with VR-O

4.4.1. Building the crude oil model system

According to the structure parameters of resin and asphaltene obtained in our experimental investigations, the constitutional repeating unit of the crude oil was constructed by using Amorphous Cell module and Dreiding force field. The viscosity difference between simulated and experimental values, $\Delta\mu$, was used to evaluate the accuracy of crude oil modeling. At 15 °C, the experimental viscosity of crude oil sample is 375 Pa s (Fig. 4b). The theoretical viscosity value from modeling using 20 structurally optimized average resin, 1 asphalene and 105 paraffin molecules (Fig. 8a) is found to be 374.89 Pa s, which is in excellent agreement with the experimental data. The simulated XRD patterns of resin and asphaltene are also shown in Fig. 8(b). The asphaltene appears to have consistent pattern compared with a typical experimental result [52,53]. Additionally, the VR-O molecules can insert into the association structures of asphaltene [54]. According to the GPC and ^{1}H NMR results of South China Sea crude oil [48], each associated asphaltene aggregate has approximately five asphaltene molecules. There are three potential insertion structures for our crude oil model system, 5-0, (the VR-O molecule is positioned on one side, while five-molecular asphaltene aggregate on the other side), 4-1 (five asphaltene aggregate molecules are isolated by the VR-O molecule, four on one side, one on the other side) and 3-2 (the VR-O molecule is inserted by splitting asphaltene aggregates into three and two molecules) (see Fig. 8c). The total energies of these model systems are 120,219.7, 233,051.3 and 74,904.3 kJ mol^{-1} for the 5-0, 4-1 and 3-2 structures, respectively. The simulation results indicate that 3-2 insertion enables the lowest total energy with the most stable structure. This implies that the 3-2 VR-O insertion into asphaltene aggregate is energetically favorable compared with those of 5-0 and 4-1. Such VR-O insertion requires energy input from external environment, such as heating and stirring. Based on the 3-2 insertion structure, the viscosity of VR-O containing model crude oil was calculated to be 218.93 Pa s, which corresponds very well with the measured value (225 Pa s). The molecular configuration of the simulated crude oil system with VR-O (see Fig. 8d) has a core constructed by asphaltene aggregate, which is covered by resin molecules and surrounded by subsequent paraffin molecules.

4.4.2. Energies of different crude oil systems

The total and non-bonding energies of different crude oil systems were calculated and listed in Table 3. The data indicate that the non-bonding energy form intermolecular interactions accounts for more than 94% of the total energy of the system, which is in agreement with previously reported results [50]. All VR-containing

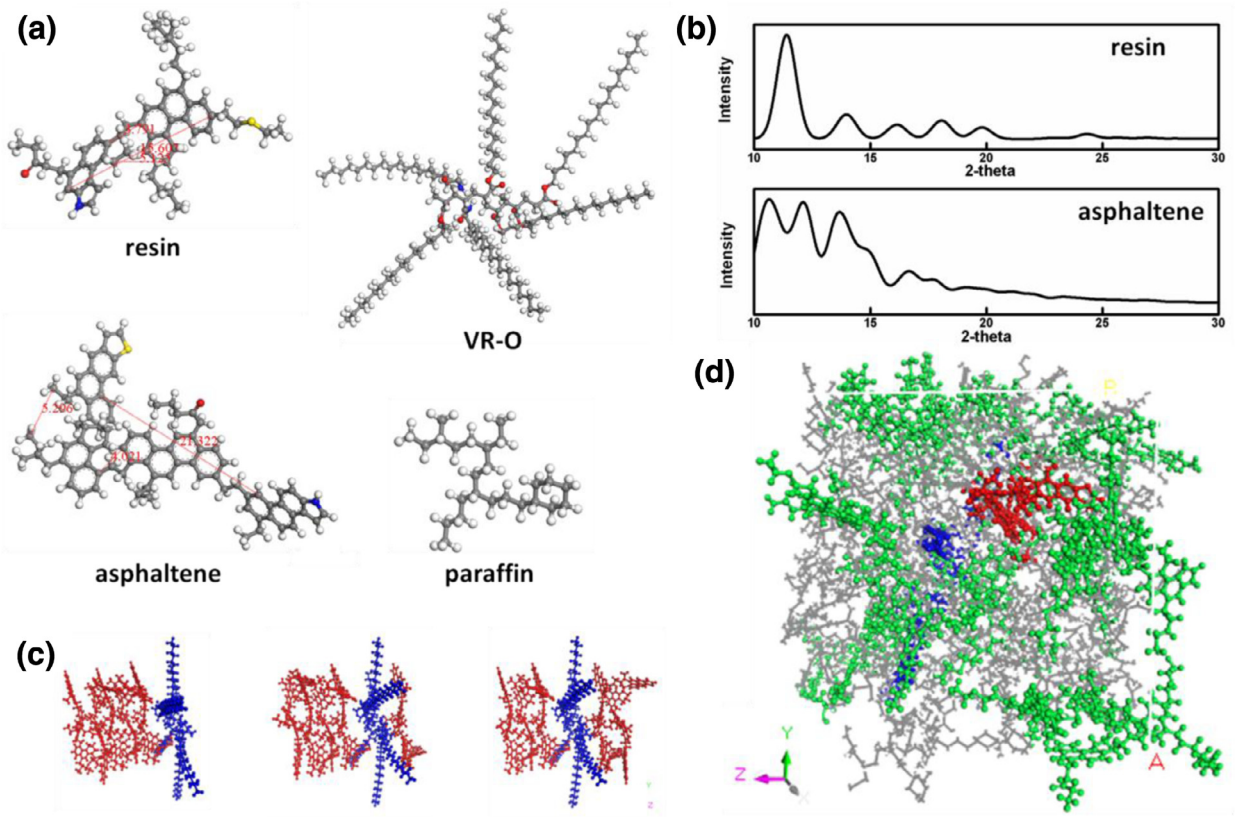

Fig. 8. (a) Structurally optimized average molecules (gray: C; white: H; red: O; yellow: S; blue: N), (b) Simulated XRD patterns, (c) insertion of VR-O into different positions of asphaltene aggregates (blue: VR-O; red: asphaltene), and (d) simulated crude oil system with VR-O (green: resin; red: asphaltene; blue: VR-O; gray: paraffin). (For interpretation of the references to color in this figure legend, the reader is referred to the web version of this article.)

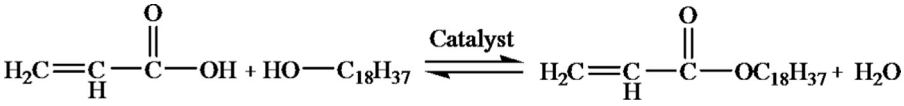

Scheme 1. Esterification reaction of 1-octadecanol and acrylic acid.

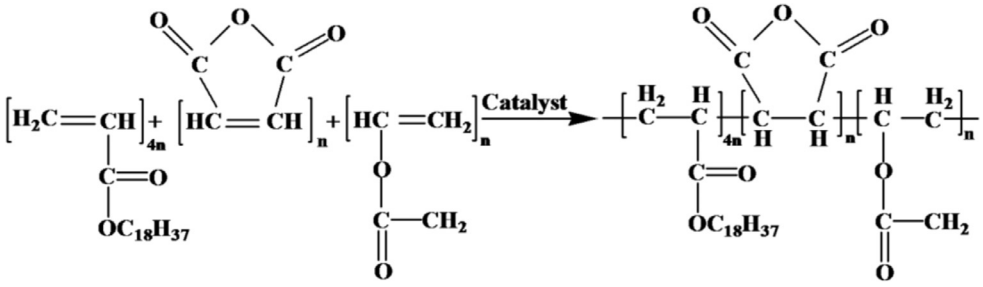

Scheme 2. Polymerization reaction.

crude oil systems show much higher energies than their corresponding VR-free systems. Higher system energy suggests that the crude oil begins to flow at lower shear stress and thus having better fluidity. The crude oil system with VR-O exhibits to be highest in total energy. This strongly supports our conclusion that introduction of VR-O leads to the best viscosity reduction performance. In addition, calculation of shear stress in each direction suggests that without and with VR-O, the shear stress values on *x*–*z* plane are 0.331 and 0.306 GPa, respectively. The reduction of 7.5% in shear stress highlights the significant effect of VR-O addition on the rheological properties of SCS crude oil. This set of computational insights further supports the conclusions from our experimental study.

5. Conclusions

The SCS crude oil was fully characterized. Its rheological properties were systematically investigated. Specifically, we synthesized several nitrogen-containing long-chain polymers, which were employed to serve as VRs to improve the fluidity of SCS crude oil. The impacts of VRs on the rheological behavior of SCS crude oil were investigated by the current combined experimental and computational study. Compositional analysis suggests that SCS crude oil has low wax content but high resin and asphaltene contents. The latter two types of compounds significantly increase the viscosity by forming association structures. In addition, SCS crude oil is found to possess thixotropy exhibiting to be a pseudoplastic fluid at

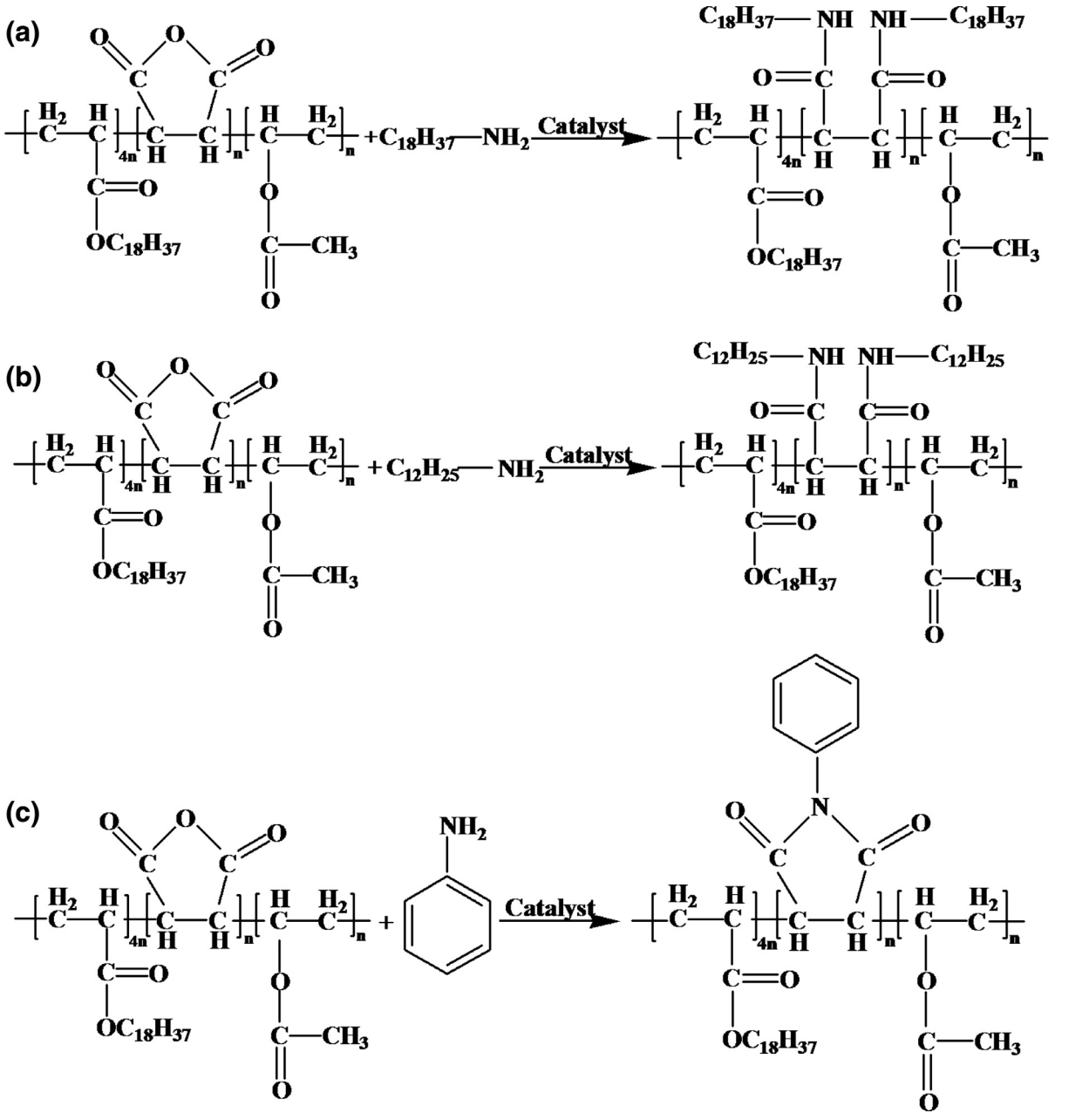

Scheme 3. Aminolysis reaction with octadecylamine (a), dodecylamine (b) and aniline (c).

Table 3. Energy of different crude oil systems.

Crude oil systems	Total energy ($\times 10^7$ kJ mol^{-1})	Non-bonding energy ($\times 10^7$ kJ mol^{-1})
VR-free	1.8914	1.7803
With VR-A	3.3570	3.2700
With VR-D	3.6466	3.5594
With VR-O	4.1189	4.0389

temperature between 15 and 25 °C. It becomes a Newtonian fluid as temperature elevates from 30 to 85 °C. All three VRs can lower the viscosity of SCS crude oil leading to improved fluidity at low temperature. The highest degree of viscosity reduction is obtained through VR-O introduction. In the presence of 1000 ppm VR-O, the viscosity of SCS crude oil is reduced by 44.2% at 15 °C and 40.2% at 40 °C, while its critical stress decreases from 590 to 370 Pa. Further, according to computational results, VR-containing crude oil has higher energy compared with its parenting VR-free sample. In other words, the VR-containing sample begins to flow at lower shear stress and thus having better fluidity. Remarkably, 7.5% reduction in shear stress highlights the crucial role of VR-O in modifying the rheological properties of SCS crude oil.

Conflict of interest

The authors declare no competing financial interest.

Acknowledgments

This work is financially supported by the Training Program of the Major Research Plan of the National Natural Science Foundation of China (grant no. 91634112), the Natural Science Foundation of Shanghai (grant no. 16ZR1408100), the Fundamental Research Funds for the Central Universities of China (grant no. 22A201514010) and the Open Project of State Key Laboratory of Chemical Engineering (SKL-ChE-16C01). D.W. acknowledges the institutional funds from the Gene and Linda Voiland School of Chemical Engineering and Bioengineering at Washington State University.

References

[1] J.G. Speight, The Chemistry and Technology of Petroleum, Marcel Dekker, New York, 1999.
[2] A. Firoozabadi, Thermodynamics of Hydrocarbon Reservoirs, McGraw-Hill, New York, 1999.
[3] J.X. Wang, J.S. Buckley, Energy Fuels 17 (6) (2003) 1445–1451.
[4] K.L. Gawrys, G.A. Blankenship, P.K. Kilpatrick, Energy Fuels 20 (2) (2006) 705–714.
[5] M. Tojima, S. Suhara, M. Imamura, A. Furuta, Catal. Today 43 (3–4) (1998) 347–351.
[6] T.G. Savvidis, D. Fenistein, L. Barre, E. Behar, AIChE J. 47 (1) (2001) 206–211.
[7] J. Tao, P. Shi, S. Fang, K. Li, H. Zhang, M. Duan, Ind. Eng. Chem. Res. 54 (17) (2015) 4851–4860.
[8] L.H. Ali, K.A. Al-Ghannam, J.M. Al-Rawi, Fuel 69 (4) (1990) 519–521.
[9] H. Groenzin, O.C. Mullins, J. Phys. Chem. A 103 (50) (1999) 11237–11245.
[10] F. Trejo, J. Ancheyta, Ind. Eng. Chem. Res. 46 (23) (2007) 7571–7579.
[11] L.V. Castro, F. Vazquez, Energy Fuels 23 (3) (2009) 1603–1609.
[12] B. Aguilera-Mercado, C. Herdes, J. Murgich, E.A. Müller, Energy Fuels 20 (1) (2006) 327–338.
[13] M. Barcenas, P. Orea, Energy Fuels 25 (5) (2011) 2100–2108.
[14] O. Leon, E. Rogel, J. Espidel, G. Torres, Energy Fuels 14 (1) (2000) 6–10.
[15] P.M. Spiecker, K.L. Gawrys, P.K. Kilpatrick, J. Colloid Interface Sci. 267 (1) (2003) 178–193.
[16] M.R. Gray, R.R. Tykwinski, J.M. Stryker, X. Tan, Energy Fuels 25 (7) (2011) 3125–3134.
[17] E. Rogel, Energy Fuels 14 (3) (2000) 566–574.
[18] Y. Zhang, T. Takanohashi, T. Shishido, S. Sato, I. Saito, R. Tanaka, Energy Fuels 19 (3) (2005) 1023–1028.
[19] F. Alvarez-Ramirez, E. Ramirez-Jaramillo, Y. Ruiz-Morales, Energy Fuels 20 (1) (2006) 195–204.
[20] O. Castellano, R. Gimon, H. Soscun, Energy Fuels 25 (6) (2011) 2526–2541.
[21] J. Zhu, S. Wei, A. Yadav, Z. Guo, Polymer 51 (12) (2010) 2643–2651.
[22] D. Zhang, A.B. Karki, D. Rutman, D.P. Young, A. Wang, D. Cocke, T.H. Ho, Z. Guo, Polymer 50 (17) (2009) 4189–4198.
[23] C. Wang, Y. Wu, Y. Li, Q. Shao, X. Yan, C. Han, Z. Wang, Z. Liu, Z. Guo, Polymer. Adv. Technol. (2017), doi:10.1002/pat.4105.
[24] Y. Zheng, Y. Zheng, S. Yang, Z. Guo, T. Zhang, H. Song, Q. Shao, Green Chem. Lett. Rev. 10 (4) (2017) 202–209.
[25] J. Zhang, Y. Liang, X. Wang, H. Zhou, S. Li, J. Zhang, Y. Feng, N. Lu, Q. Wang, Z. Guo, Adv. Compos. & Hy. Mater. (2017).
[26] A. Borthakur, D. Chanda, S.R.D. Choudhury, K.V. Rao, B. Subrahmanyam, Energy Fuels 10 (3) (1996) 844–848.
[27] S. Sharma, V. Mahto, V.P. Sharma, Ind. Eng. Chem. Res. 53 (12) (2014) 4525–4533.
[28] S.W. Hasan, M.T. Ghannam, N. Esmail, Fuel 89 (5) (2010) 1095–1100.
[29] R. Tao, X. Xu, Energy Fuels 20 (5) (2006) 2046–2051.
[30] J.L. Gonçalves, A.J.F. Bombard, D.A.W. Soares, G.B. Alcantara, Energy Fuels 24 (5) (2010) 3144–3149.
[31] S.K. Maity, J. Ancheyta, G. Marroquín, Energy Fuels 24 (5) (2010) 2809–2816.
[32] H. Wang, Y. Wu, L. He, Z.W. Liu, Energy Fuels 26 (11) (2012) 6518–6527.
[33] X. Song, H. Yin, Y. Feng, S. Zhang, Y. Wang, Ind. Eng. Chem. Res. 55 (23) (2016) 6563–6568.
[34] L.V. Castro, F. Vazquez, Energy Fuels 22 (6) (2008) 4006–4011.
[35] T.E. Chávez-Miyauchi, L.S. Zamudio-Rivera, V. Barba-López, Energy Fuels 27 (4) (2013) 1994–2001.
[36] J. Xu, H.J. Jiang, T. Li, X.M. Wei, T.S. Wang, J. Huang, W.N. Wang, A.L. Smith, J. Wang, R. Zhang, Y.S. Xu, L. Li, R.K. Prud'homme, X.H. Guo, Ind. Eng. Chem. Res. 54 (19) (2015) 5204–5212.
[37] L.A. Alcazar-Vara, L.S. Zamudio-Rivera, E. Buenrostro-Gonzaĺez, Ind. Eng. Chem. Res. 54 (32) (2015) 7766–7776.
[38] C. Baudilio, M. Carmen, L.P. Jose´, J.E. Juan, D.R. María, Fuel 87 (10–11) (2008) 2090–2094.
[39] B. Coto, J.A.P. Coutinho, C. Martos, M.D. Robustillo, J.J. Espada, L.J. Pena, Energy Fuels 25 (3) (2011) 1153–1160.
[40] Z. Guo, H.W. Ng, G.L. Yee, H.T. Hahn, J. Nanosci. Nanotechnol. 9 (2009) 3278–3285.
[41] Z. Sum, L. Zhang, F. Dang, Y. Liu, Z. Fei, Q. Shao, H. Lin, J. Guo, L. Xiang, N. Yerra, Z. Guo, CrystEngComm 19 (2017) 3288–3298.
[42] Y. Cao, J. Huang, Y. Li, S. Qiu, J. Liu, A. Khasanov, M.A. Khan, D.P. Young, F. Peng, D. Cao, X. Peng, K. Hong, Carbon 109 (2016) 640–649.
[43] Y.H. Zhang, L.F. Han, Y.H. Xiao, D.Z. Jia, Z.H. Guo, F. Li, Comput. Mater. Sci. 69 (2013) 222–228.
[44] J. Liu, Y. Gao, D. Cao, L. Zhang, Z. Guo, Langmuir 27 (12) (2011) 7926–7933.
[45] Y. Gao, J. Liu, J. Shen, L. Zhang, Z. Guo, D. Cao, Phys. Chem. Chem. Phys. 16 (2014) 16039–16048.
[46] M.D.A. Hasan, M. Fulem, A. Bazyleva, J.M. Shaw, Energy Fuels 23 (10) (2009) 5012–5021.
[47] K. Paso, A. Silset, G. Sørland, M.A.L. Gonçalves, J. Sjoblom, Energy Fuels 23 (1) (2008) 471–480.
[48] H.R. Zhang, B.X. Shen, H. Sun, J.C. Liu, Pet. Process. Petrochem. 46 (12) (2015) 31–40.
[49] D. Merino-Garcia, S.I. Andersen, Langmuir 20 (11) (2004) 4559–4565.
[50] P. Wang, Z. Dong, Y. Tan, Z. Liu, Energy Fuels 29 (1) (2015) 112–121.
[51] C.X. Li, Z.M. Luo, Rheology and Measurement of Crude Oils, China University of Petroleum Press, Dongying, China, 1994.
[52] J. Christopher, A.S. Sarpal, G.S. Kapur, A. Krishna, B.R. Tyagi, M.C. Jain, S.K. Jain, A.K. Bhatnagar, Fuel 75 (8) (1996) 999–1008.
[53] J. Shirokoff, M.N. Siddiqui, M.F. Ali, Energy Fuels 16 (3) (1997) 561–565.
[54] V. Meyer, J. Pilliez, J.P. Habas, F. Montel, P. Creux, Energy Fuels 22 (5) (2008) 3154–3159.
[55] L.W. Ali, K.A. Al-Ghannam, Fuel 60 (11) (1981) 1043–1046.